THE ASTROPHYSICAL JOURNAL, 203:151–158, 1976 January 1

OBSERVATIONS OF THE GUM NEBULA WITH A FABRY-PEROT SPECTROMETER

R. J. REYNOLDS
Physics Department, University of Wisconsin, Madison
Received 1975 March 24; revised 1975 June 13

ABSTRACT

Scans have been made of Hα, [N II] λ6584, [O III] λ5007, and He I λ5876 in selected directions in the Gum Nebula. Analyses of the line profiles and line intensities indicate that much of the emitting gas in the Gum Nebula is confined to an expanding shell which has a radius of about 125 pc, an expansion velocity of approximately 20 km s^{-1}, an emission measure which ranges from about 15 cm^{-6} pc to about 500 cm^{-6} pc, and a temperature near 11,000 K. The ultraviolet ($h\nu > 13.6$ eV) flux from ζ Pup and γ^2 Vel appears to be capable of producing most of the observed ionization, although the origin of the shell structure and high expansion velocity is not certain.

Subject headings: interstellar: matter — nebulae: individual

I. INTRODUCTION

The Gum Nebula is a very large region of ionized gas first observed by Colin Gum (1955) during an Hα photographic survey of H II regions in the Southern Milky Way. Subsequently, there has been considerable controversy about the origin of the nebula and the source of its ionization. Some (Beuermann 1973; Gum 1956) have suggested that the Gum Nebula is an extended H II region ionized by ultraviolet radiation from hot stars located within the nebula, particularly ζ Pup, an O5 star, and γ^2 Vel, a Wolf-Rayet star with an O star companion. Others (Brandt *et al.* 1971; Alexander *et al.* 1971) have argued that the ultraviolet radiation from these stars is not sufficient to produce the observed ionization. They have suggested instead that the Gum Nebula may be a hot ($T \gtrsim 40{,}000$ K), highly ionized, "fossil Strömgren sphere" which was initially heated and ionized by a supernova burst and is now in the process of cooling and recombining.

In order to help determine the dominant source of the heating and ionization of the nebula, a Fabry-Perot spectrometer was used to measure the intensities, widths, and radial velocities of Hα, [N II], and [O III] emission lines in selected directions in the nebula. These observations have yielded information about the temperature, kinematics, and spatial structure of the emitting gas.

II. OBSERVATIONS

Figure 1 shows part of a recent Hα photographic survey of the galactic plane by J. P. Sivan (1974) which includes the region of the galactic plane in which the Gum Nebula is located. The Hα emission associated with the Gum Nebula appears to be confined to a nearly circular region approximately 36° in diameter which is located between galactic longitudes 240° and 276° and galactic latitudes −19° and +17°. The diameter of the Gum Nebula, assuming a distance to its center of 400 ± 60 pc (Brandt *et al.* 1971; Gott and Ostriker 1971), is therefore approximately 250 pc. The Hα emission along the galactic equator at longitudes greater than 283° is apparently associated with H II regions in the Carina arm of the Galaxy (e.g., the η Carinae nebula at $l = 288°$ and the m Centauri nebula at $l = 306°$ [Sivan 1974]).

Using a 15 cm diameter, two-etalon Fabry-Perot spectrometer at the focus of the 60-inch (1.5 m) primary of the McMath solar telescope at Kitt Peak National Observatory, scans were obtained of Hα, [N II] λ6584, [O III] λ5007, and He I λ5876 in selected directions in the nebula. The eight observation directions are labeled A through H on Figure 1 and run approximately from north to south through the nebula: direction A is well outside the main Hα emission region, B is on the relatively bright northern rim, directions C, D, E, and F sample the fainter interior regions of the nebula, while G and H are in the brighter southern parts of the nebula, 0°.4 from ζ Pup and 1°.1 from γ^2 Vel, respectively. The altitude above the horizon for these observations ranged from about 10° to about 30°.

The field of view of the spectrometer was 5'.7 and the radial velocity resolution was approximately 12 km s^{-1}. This velocity resolution made it possible to study the kinematics of the emitting gas from the structure of the observed emission-line profiles.

As an example of the data which have been obtained, scans of Hα, [N II], and [O III] for directions D and G have been plotted in Figure 2. The scans on the left are essentially the "raw" data which consist of photomultiplier counts accumulated in 2.07 km s^{-1} velocity bins plotted versus radial velocity with respect to the local standard of rest. The solid curve drawn through the data points is a computer fit of the emission profile obtained by assuming that the profile is composed of Gaussian emission-line components which have been broadened by the instrumental response function. On the right side of Figure 2 are plotted the computer-fitted galactic emission-line profiles with instrumental broadening removed. The

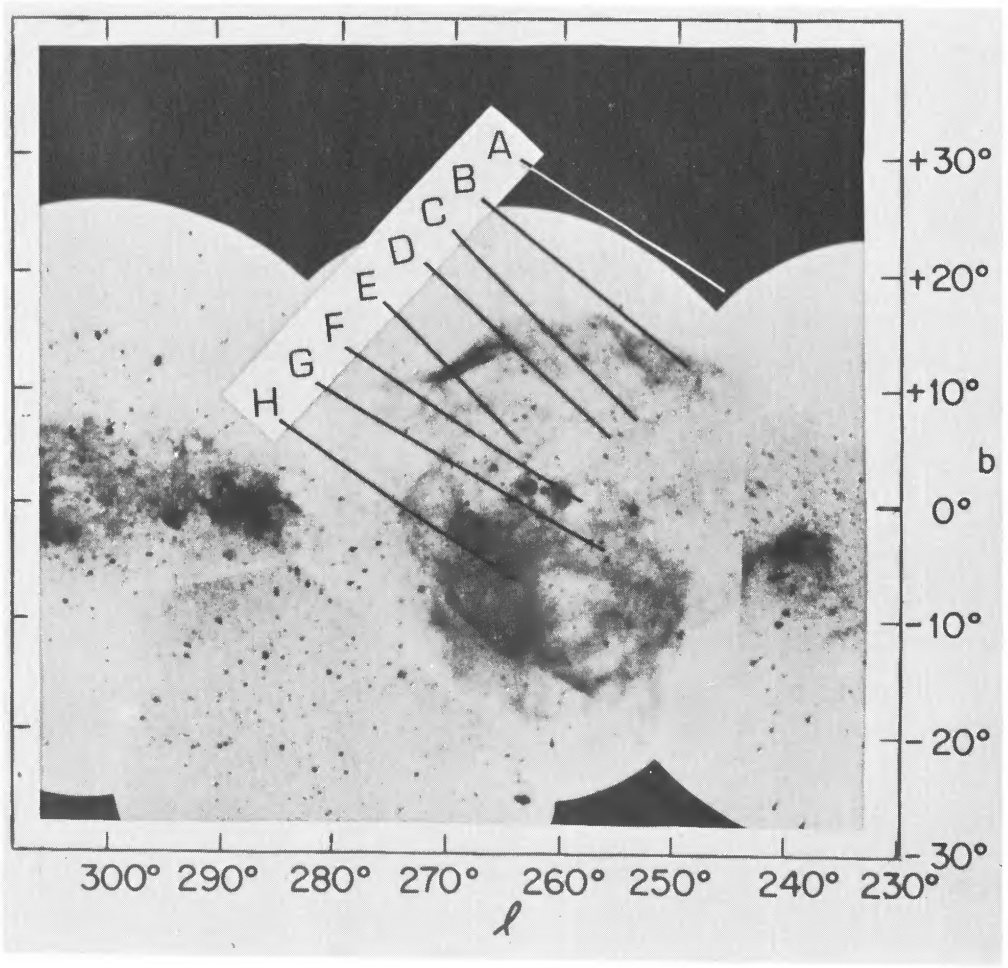

FIG. 1.—A wide-angle Hα photograph of the Gum Nebula by J. P. Sivan (1974). The Fabry-Perot observation directions are at the end points of the straight lines. ζ Pup and γ^2 Vel are 0°.4 and 1°.1 from directions G and H, respectively. Reproduced courtesy of *Astronomy and Astrophysics*.

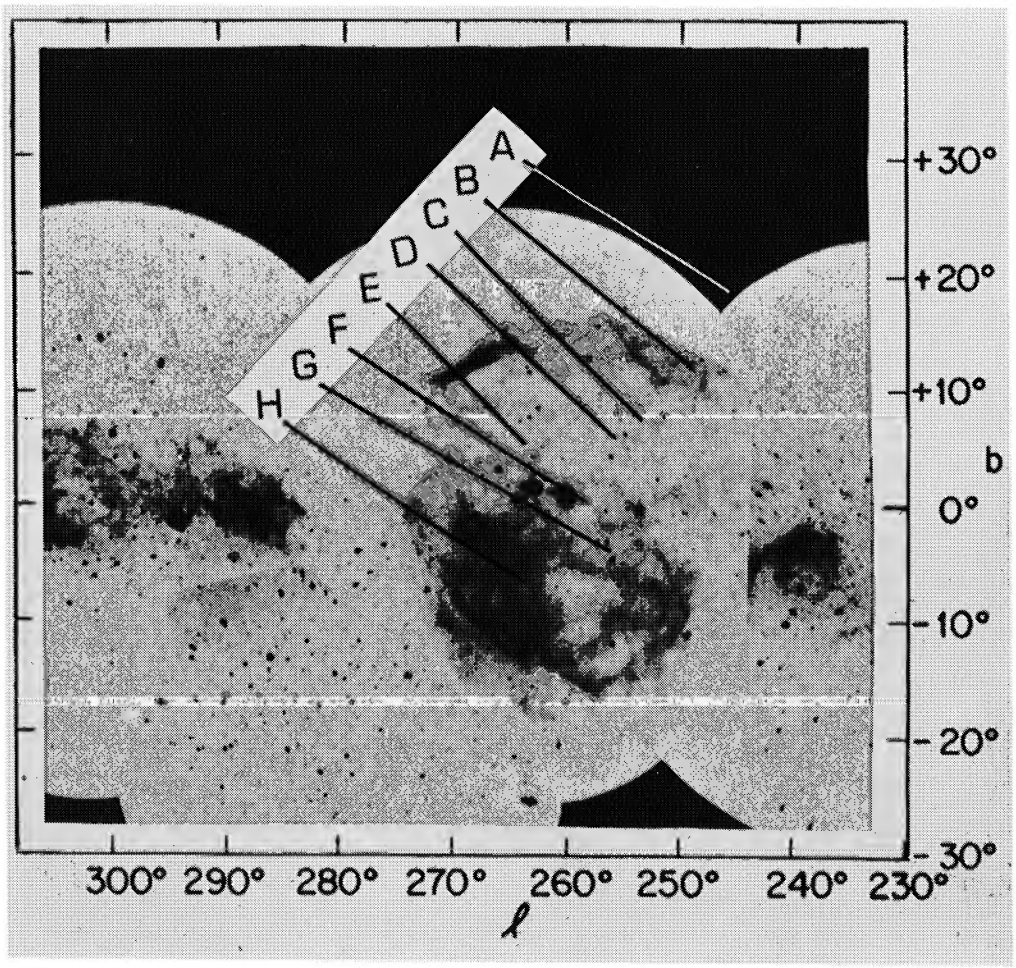

FIG. 1.—A wide-angle Hα photograph of the Gum Nebula by J. P. Sivan (1974). The Fabry-Perot observation directions are at the end points of the straight lines. ζ Pup and γ^2 Vel are 0°.4 and 1°.1 from directions G and H, respectively. Reproduced courtesy of *Astronomy and Astrophysics*.

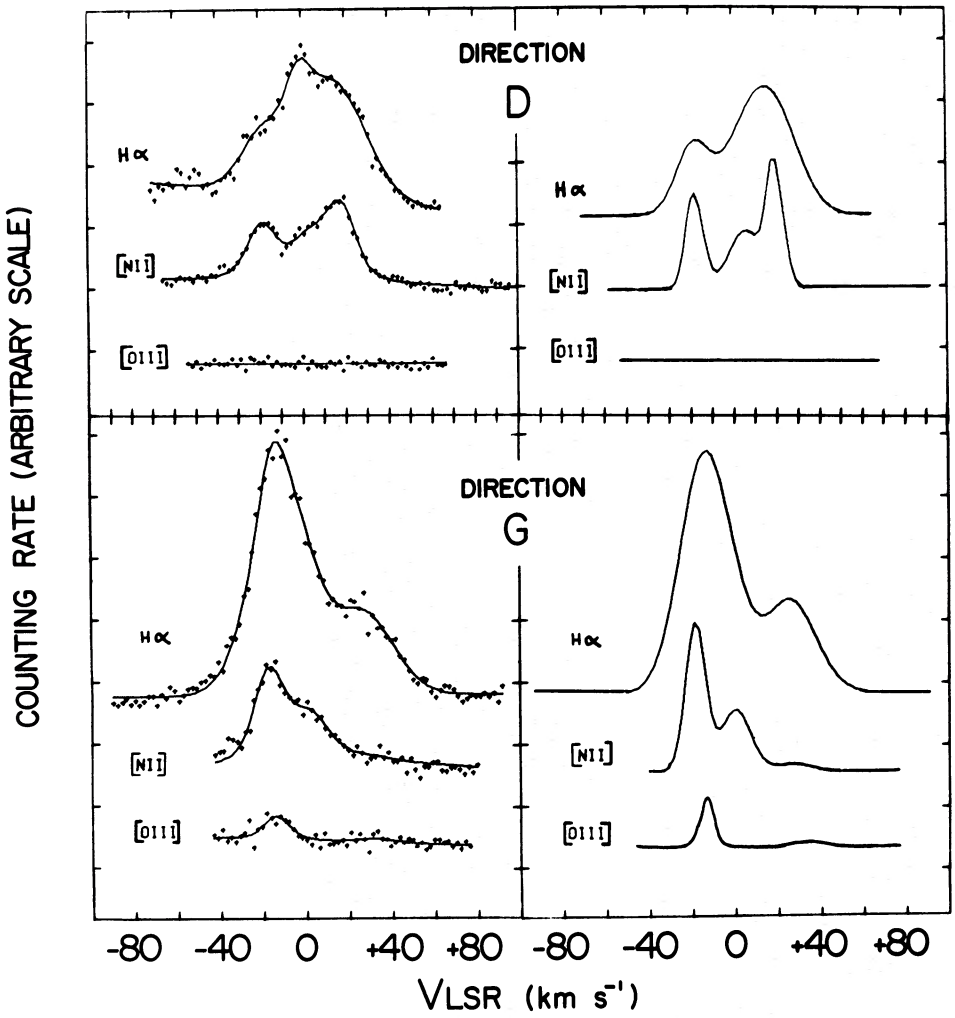

FIG. 2.—Scans of Hα, [N II] λ6584, and [O III] λ5007 in directions D and G. The scans on the left are the "raw" data, while the scans on the right are the computer-fitted galactic emission profiles with instrumental broadening removed. Geocoronal Hα has been subtracted from the computer-fitted Hα profiles.

the peaks of the hydrogen components, the open circles denote the nitrogen line velocities, and the crosses give the positions of the observed oxygen lines. The solid horizontal bars through the data points denote the full widths at half-maximum (FWHM) of the hydrogen and nitrogen emission line components. The dotted vertical line represents the expected velocity of the Gum Nebula's standard of rest, which is shifted with respect to the LSR velocity by galactic differential rotation. Except for directions B and F, the nebular emission profiles appear to be split into two principal velocity components separated by up to 45 km s^{-1}, with one component to the blue and the other component to the red of the Gum Nebula's standard of rest. This suggests that the emitting gas is confined to an expanding shell with an expansion velocity of approximately 20 km s^{-1}. The expansion velocities appear to be larger on the average for the fainter portions of the shell than for the brighter (and perhaps more massive) portions of the shell. For example, in directions C, D, E, and G, the Hα component with the larger radial velocity with respect to the Gum Nebula's standard of rest is always the component with the smaller emission measure.

For a given principal velocity component, there appear to be no significant differences between the radial velocities of the hydrogen, nitrogen, and oxygen emission lines.

The thickness and electron density of the shell can be estimated by comparing the emission measure with the pulsar dispersion measure DM in the directions of pulsars located within the nebula. Assuming the shell has a thickness L and a uniform electron density n_e along a line of sight through the shell, and assuming the dispersion measures are produced primarily by the emitting gas within the shell, then

$$L \approx \frac{(\mathrm{DM})^2}{\mathrm{EM}}, \qquad (4)$$

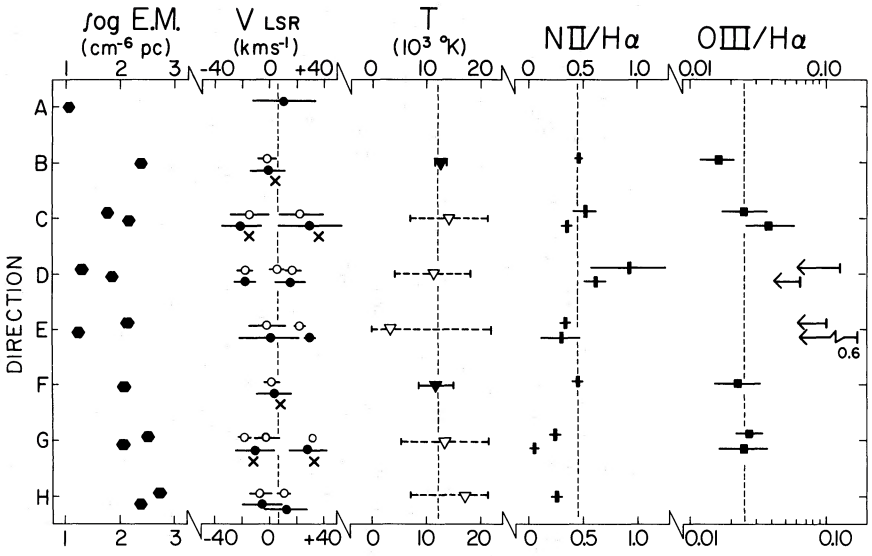

FIG. 3.—A summary of results for the eight observation directions. Plotted are: the logarithm of the emission measure for each velocity component, the radial velocity and FWHM for each observed emission line (●–Hα; ○–[N II]; ×–[O III]), the derived temperatures, and the [N II] λ6584/Hα and [O III] λ5007/Hα intensity ratios (energy units). The value for the negative principal velocity component is plotted slightly above the value for the positive component in a given direction.

and

$$n_e = \frac{\mathrm{EM}}{\mathrm{DM}}, \tag{5}$$

where EM is the emission measure computed from the blue Hα emission component. For pulsars located behind the nebula, EM is obtained from the sum of the two emission components, and the resulting shell thickness L is given by $(\mathrm{DM})^2/2$ EM instead of equation (4). There are three pulsars in the direction of the Gum Nebula: MP 0736, PSR 0833 (the Vela pulsar), and MP 0835, which are all located in the brighter southern portion of the nebula. Although no scans were taken in the directions of these pulsars, emission measures were estimated from Sivan's (1974) Hα photograph (Fig. 1) using the Hα observations in directions G and H (which were within about 5° of the pulsars) as a calibration. If PSR 0833 is located within the nebula and MP 0736 and MP 0835 are located behind the nebula (Brandt 1971), then

$$L \approx 30\text{–}15 \text{ pc} \ (\approx 20\% \text{ of the nebular radius}),$$

and

$$n_e \approx 2.5\text{–}5.0 \text{ cm}^{-3}.$$

These values for L are consistent with values for the shell thickness estimated from the width of the ridge of enhanced Hα emission along the nebula's northern boundary (see Fig. 1).

Assuming a uniform shell thickness, these results imply $n_e \approx 1 \text{ cm}^{-3}$ in the fainter regions of the nebula. Fluctuations in the electron density along a line of sight through the shell will result in average electron densities within the shell that are less than the above values for n_e and a shell thickness that is greater than the above value for L. The presence of additional regions of ionization along the line of sight which do not emit detectable optical emission lines would have the opposite effects on n_e and L. Neglecting these effects, the shell is estimated to have a mass of 7–50 × $10^4 M_\odot$ and a kinetic energy of expansion of 1.5–15 × 10^{50} ergs.

c) *Temperature and Turbulence*

The Hα component line widths are observed to be systematically larger than the corresponding [N II] component line widths (Fig. 3, col. [2]). Assuming that the hydrogen and nitrogen lines are emitted by the same gas (i.e., the H^+ and N^+ ions have the same temperature and turbulent velocity distribution), and assuming that the turbulent velocity distribution (which may include differential expansion of the shell as well as smaller scale random motions of the gas) is Gaussian, then this observed difference between the random velocities of H^+ and the more massive N^+ ions can be used to determine separately the temperature and turbulent velocities of the gas. The temperature T and the FWHM V_T of the turbulent velocity distribution are then given by the relations

$$T(\mathrm{K}) = 23.5 W_{\mathrm{H}}^2 \left(1 - \frac{W_{\mathrm{N}}^2}{W_{\mathrm{H}}^2}\right), \tag{6}$$

$$V_T(\mathrm{km\ s^{-1}}) = 1.04 W_{\mathrm{N}} \left(1 - 0.071 \frac{W_{\mathrm{H}}^2}{W_{\mathrm{N}}^2}\right)^{1/2}, \tag{7}$$

where W_{H} and W_{N} are the FWHMs (instrumental broadening removed) of the Hα and [N II] lines, respectively, expressed in units of km s^{-1}. For most of the cases considered, the temperatures and turbulent velocities were such that the widths of the hydrogen

lines were produced primarily by thermal motions, while the widths of the nitrogen lines were produced primarily by turbulent motions. Therefore, since good fits were obtained by assuming Gaussian line shapes for both the hydrogen and nitrogen emission components, both thermal and turbulent velocity distributions must be approximately Gaussian (as was assumed above). Deviations of the turbulent velocity distribution from a Gaussian would have resulted in underestimates of T using equation (6), which could be at most about 25 percent.

Since the Hα recombination line is actually composed of two fine-structure components separated by 4.8 km s^{-1} (0.105 Å), the Hα line profiles cannot be truly Gaussian. However, for the Hα lines that were observed, the non-Gaussian distortion produced by fine structure is small. Consideration of this additional nonthermal contribution to the width of the Hα line results in a temperature which is about 7 percent lower than that derived directly from equation (6).

Temperatures derived using equation (6) have been plotted in the third column of Figure 3. The solid triangles refer to temperatures derived in directions where only single-Gaussian nebular Hα and [N II] emission components were observed. In the other directions, where the galactic emission consists of blended multiple Gaussian components, an average temperature for the components could be determined more accurately than individual component temperatures. This is due to the fact that the sum of the squares of the component widths is less sensitive to the fit than the square of the individual widths. These average temperatures are denoted by the open triangles. The error bars on the open triangles denote my estimate of the maximum error in the result; the error bars on the solid triangles denote $\pm 1\,\sigma$ errors calculated by the fitting program.

Derived temperatures range from 3000 K to 17,000 K, and the results are consistent with a uniform temperature throughout the nebula of 11,300 K, which is obtained from a least-squares fit of the data in Figure 3 plus a correction for the effect of Hα fine structure.

The derived turbulent velocities are listed in Table 1. Parentheses indicate values for V_T which are an average for the observed velocity components. In direction A the [N II] emission was very faint and nearly obscured by a broad airglow feature, and therefore neither T nor V_T could be determined. The high turbulent velocity in direction C may indicate the presence of additional unresolved velocity components.

TABLE 1

TURBULENT VELOCITY WIDTHS (FWHM)

Direction	l	b	V_T (km s^{-1})
A.....	246.2	+19.0	...
B.....	249.2	+12.2	13 ± 1
C.....	253.3	+ 8.5	(32 ± 4)
D.....	255.6	+ 6.4	(7 ± 3)
E.....	263.8	+ 6.0	(20 ± 10)
F.....	258.4	+ 1.1	10 ± 1
G.....	255.8	− 4.4	(15 ± 8)
H.....	263.7	− 7.0	(10 ± 6)

d) Line Intensity Ratios

The observed [N II] λ6584/Hα and [O III] λ5007/Hα intensity ratios are given in the last two columns of Figure 3. A [N II]/Hα ratio of 0.45 is consistent with the observations in the first five directions within the nebula (B through F), although there is evidence that the ratio may be significantly lower in the two directions near ζ Pup and γ^2 Vel (G and H, respectively). Using the relationship between the volume densities $n(H^+)$ and $n(N^+)$ and the [N II]/Hα intensity ratio given by Burbidge *et al.* (1963), and using a temperature of 11,300 K, then

$$\frac{n(N^+)}{n(H^+)} = 2.0 \pm 0.7 \times 10^{-5}$$

for directions B through F; the ratio is perhaps a factor of 2 smaller in directions G and H. Assuming that the hydrogen within the emitting regions is nearly fully ionized and that nitrogen is predominantly in the N^+ ionization state, these results suggest that nitrogen is underabundant by about a factor of 4 (direction B through F) to 9 (directions G and H) with respect to its "cosmic" abundance (Allen 1963). This apparent underabundance of nitrogen is consistent with the findings of Burton *et al.* (1974), who analyzed ultraviolet absorption lines in the spectra of ζ Pup and γ^2 Vel. However, a systematic error in the determination of T from the line profiles could also produce the low value for the $n(N^+)/n(H^+)$ ratio given above, and forcing the abundance ratio to be near "cosmic" would only require lowering the gas temperature from 11,000 K to near 8,000 K. Such an error would occur, for example, if the nitrogen emission were produced in systematically less turbulent and/or cooler regions than the Hα emission. However, at present there is no evidence for such an effect.

The last column of Figure 3 lists the measured [O III] λ5007/Hα intensity ratios. An average value of $2.4 \pm 0.5 \times 10^{-2}$ is consistent with all the observations, although higher values may be allowed in directions D and E where only upper limits could be determined. Assuming a "cosmic" abundance for oxygen (Allen 1963) and a temperature of 11,300 K, these observations imply that only 10^{-3} to 10^{-2} of the oxygen atoms within the emitting regions are in the O^{++} ionization state.

Scans were also made of the spectral region around He I λ5876. Unfortunately this spectral region is contaminated by unidentified airglow emission features which had greater intensities than the Gum Nebula He I emission. As a result, He I emission was only marginally detected in three directions (B, G, and H). A He I λ5876/Hα intensity ratio of $4 \pm 3 \times 10^{-2}$ is consistent with these observations.

IV. SUMMARY AND DISCUSSION

These results indicate that much of the emitting gas in the Gum Nebula is confined to an expanding shell

which has a thickness of about 20 percent of the nebular radius, a radial expansion velocity of approximately 20 km s^{-1}, an average electron density which ranges from about 1 cm^{-3} to about 5 cm^{-3}, and a temperature near 11,000 K. The ultraviolet ($h\nu >$ 13.6 eV) flux from ζ Pup and γ^2 Vel appears to be capable of maintaining the observed ionization.

These optical observations do not provide any evidence for the existence of the higher temperature ($T \gtrsim$ 40,000 K) component of the Gum Nebula predicted by the "fossil Strömgren sphere" model. Because O II atoms have a relatively high ionization potential (35 eV) compared with hydrogen and nitrogen (14 eV), [O III] emission is expected to be preferentially produced in hotter, higher excitation regions. However, the relatively faint [O III] λ5007 emission that is observed appears to be associated (kinematically at least) with the 11,000 K gas rather than with any hotter component; furthermore, the measured FWHM of 8 ± 5 km s^{-1} for the -11 km s^{-1} [O III] line in direction G (the brightest observed [O III] line) is consistent with a temperature $T <$ 20,000 K for the emitting O III atoms. Any additional (hotter) source of [O III] emission in directions B through G must have an [O III] λ5007 intensity $\lesssim 1 \times 10^{-6}$ ergs cm^{-2} s^{-1} sr^{-1}. It should be emphasized that these observations do not exclude the existence of a gas with $T > 10^5$ K, since most of the oxygen atoms at those temperatures would be in ionization states higher than O III. Observations of O VI absorption lines in the directions of ζ Pup and γ^2 Vel by *Copernicus* (York 1974; Jenkins and Meloy 1974) do in fact suggest the presence of such a gas along the line of sight. However, since O VI absorption lines were also detected in many other directions in the Galaxy, the relationship (if any) between this very hot gas and the Gum Nebula is uncertain.

These findings appear to be more consistent with the conclusions of Beuermann (1973) who, after a reexamination of the earlier optical and radio observations, concluded that the ionized gas associated with the Gum Nebula has an angular radius of about 18° and a temperature $\lesssim 10^4$ K. Beuermann also suggested that the Gum Nebula may be an old H II region with a shell structure that had formed as a result of evolutionary expansion. However, in models of evolved H II regions (Lasker 1966), the ionized gas attains an expansion velocity of only about 4 km s^{-1}, and also remains rather uniformly distributed throughout the volume of the H II region. The models do predict the formation of a higher velocity, more dense outer shell, but this shell is composed of neutral rather than ionized gas. Therefore, while the ionization and temperature of the emitting gas in the Gum Nebula can probably be accounted for by the ultraviolet flux from ζ Pup and γ^2 Vel, the origin of its shell structure and high expansion velocities is not yet certain.

I am greatly indebted to F. L. Roesler who carried out some of these observations. I also thank F. Scherb for helpful discussions, and D. Huppler, J. Trauger, F. Barmore, D. Cox, M. Kafatos, and D. Evans for their assistance. This work has been supported by the Astronomical Instrumentation section of the National Science Foundation through grant GP-43932, Kitt Peak National Observatory, the University of Wisconsin Graduate School, the Planetary Astronomy Program of the National Aeronautics and Space Administration through grant NGR 50-002-242, and the Aeronomy section of the National Science Foundation through grant GA-40146.

REFERENCES

Alexander, J. K., Brandt, J. C., Maran, S. P., and Stecher, T. P. 1971, *Ap. J.*, **167**, 487.
Allen, C. W. 1963, *Astrophysical Quantities* (2d ed.; London: Athlone Press).
Beuermann, K. P. 1973, *Ap. and Space Sci.*, **20**, 27.
Brandt, J. C. 1971, *The Gum Nebula and Related Problems*, ed. S. P. Maran, J. C. Brandt, and T. P. Stecher (Proceedings of a Symposium at Goddard Space Flight Center, NASA SP-332), p. 4.
Brandt, J. C., Stecher, T. P., Crawford, D. L., and Maran, S. P. 1971, *Ap. J. (Letters)*, **163**, L99.
Burbidge, G. R., Gould, R. J., and Pottasch, S. R. 1963, *Ap. J.*, **138**, 945.
Burton, W. M., Evans, R. G., and Griffin, W. G. 1974, *M.N.R.A.S.*, **169**, 307.
Conti, P. S. 1973, *Ap. J.*, **179**, 181.
Gott, J. R., III, and Ostriker, J. P. 1971, *The Gum Nebula and Related Problems*, ed. S. P. Maran, J. C. Brandt, and T. P. Stecher (Proceedings of a Symposium at Goddard Space Flight Center, NASA SP-332), p. 42.
Gum, C. S. 1955, *Mem. R.A.S.*, **67**, 155.
———. 1956, *Observatory*, **76**, 150.
Ishida, K., and Kawajiri, N. 1968, *Publ. Astr. Soc. Japan*, **20**, 95.
Jenkins, E. B., and Meloy, D. A. 1974, *Ap. J. (Letters)*, **193**, L121.
Lasker, B. M. 1966, *Ap. J.*, **143**, 700.
Reynolds, R. J., Roesler, F. L., and Scherb, F. 1974, *Ap. J. (Letters)*, **192**, L53.
Sivan, J. P. 1974, *Astr. and Ap. Suppl.*, **16**, 163.
Torres-Peimbert, S., Lazcano-Araujo, A., and Peimbert, M. 1974, *Ap. J.*, **191**, 401.
York, D. G. 1974, *Ap. J. (Letters)*, **193**, L127.

RONALD J. REYNOLDS: Space Physics Laboratory, University of Wisconsin, 1150 University Avenue, Madison, WI 53706